384 Element Si Detector Characterization and Comparison with 13 Element Canberra Ge Detector

The 384 element diode array detector comprised the first major component of the development project. This detector was commissioned and extensively tested during this second year of the grant. The comprehensive set of MCA profiles for the detector for all in put photon rates can be found at the web site http://web.njit.edu/~tyson/Detector_384_Sept2009_MCA_Profiles/. For low count rates (~6 cps per channel) the response was tested using a Fe^{55} radioactive source and yielded a resolution of ~300 eV. See Figs. 2.1 to 2.5 for the details.

Using a Cu foil as a source and fixing the incident energy at 9100 eV (at the X11B beamline) the detector element profiles were examined for a large range of input photon intensities (labeled by the ion chamber intensity). At 2μs shaping time linearity is maintained up to ~50,000 per channel. For rates up to 50,00- cps the resolution varies up from ~300 to ~370 eV. At 0.5 μs shaping time small deviations are found from linearity for rates up to 150,000 cps pre channel. Also, the energy resolution is essentially constant at ~350 eV up to a maximum counting rate of 200,000 cps per channel. For this shaping time (See Figs.2.6 to 2.9). For the 2 μs curve good resolution and position stability of the emission line will be maintained away from the white line in the XAFS region where is no large change in fluorescence counts (rates below 50,000 cps per channel, see Fig. 2.7). The 0.5 and 1 μs peak positions curves are very stable to very high counting rates on the other hand. **For systems with high fluorescence signals, operating the detector at a 0.5 μs shaping times will provide a good compromise of 350 eV resolution and high counting rates with no drift in emission line positions. For dilute systems with low fluorescence signals, using 2 μs shaping time will yield resolution equivalent to a commercial Ge detector but with much higher total counting rate capability (as in the Mn doped Ge system below).**

A real sample was examined with the detector. This sample was a 100 nm magnetic semiconductor film of Ge0.98Mn0.02 on a GaAs. The low level of Mn was used to test the noise level in the detector (see Fig. 2.10 and 2.11). Comparison was made to a standard 13 element Canberra detector used on the same sample. The 384 element detector had a resolution of 274 eV compared to the 13 element Ge detector which had a resolution of 248 eV. The results show that the detector will perform extremely well for these types of experiments.

In summary the detctor is capable of operation at a counting rate of 50,000 cps per channel and ~300 to 375 eV (depending on counting rate) resolution in the linear regime for a total rate of ~19 MHz (2 μs shaping time) or can operate up to 150,000 cps per channel with an essentially constant resolution of ~ 350 eV (0.5 μs shaping time) giving a total counting rate of ~57 MHz. Modest deadtime corrections will be required at the higher counting rates. The detector will be used on X14A in x-ray holography experiments and at X11B for x-ray spectroscopic measurements.

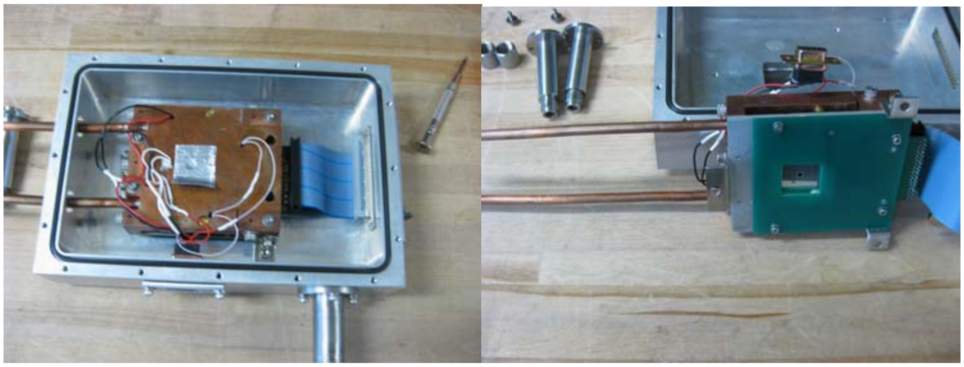

Fig.2.1. Packaging for diode-base 384 element detector showing heat sink and chiller tubing. In operations the circulating coolant is at 5° C and the detector elements are kept at -42°C with thermoelectric coolers. The case is continuously vacuum pumped to a pressure below 10^{-6} mbar.

Fig.2.2. Each element (diode) is 1 mm x 1mm and the arrangement is a 20 x 20 square. There is a hole in the middle of the array for beam pass-through omitting a 4 x 4 array (hence there are 384 elements). This hole can be used for normal incidence measurements with a modified detector casing.

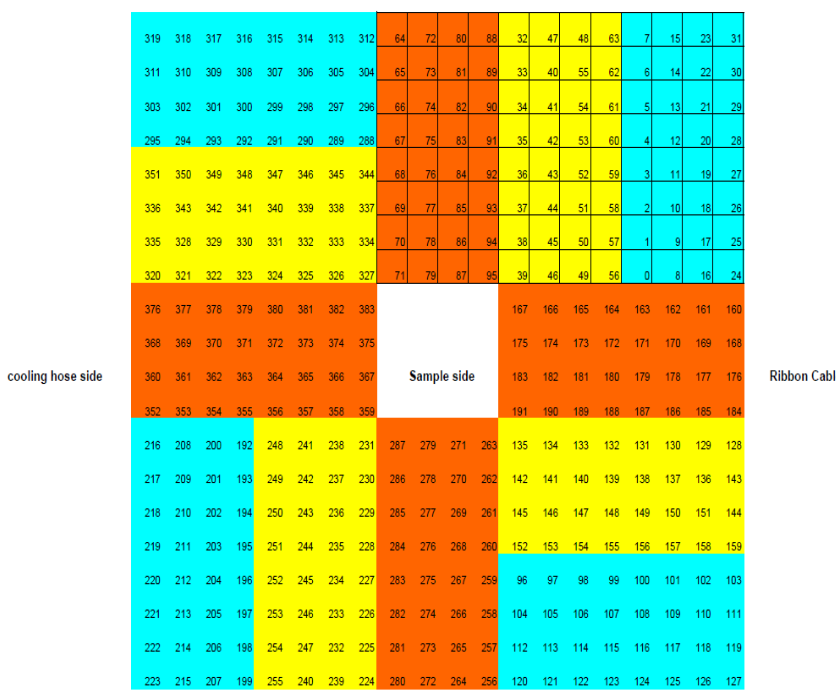

Fig. 2.3. Schematic with labels for the 384 Detector elements.

(a)
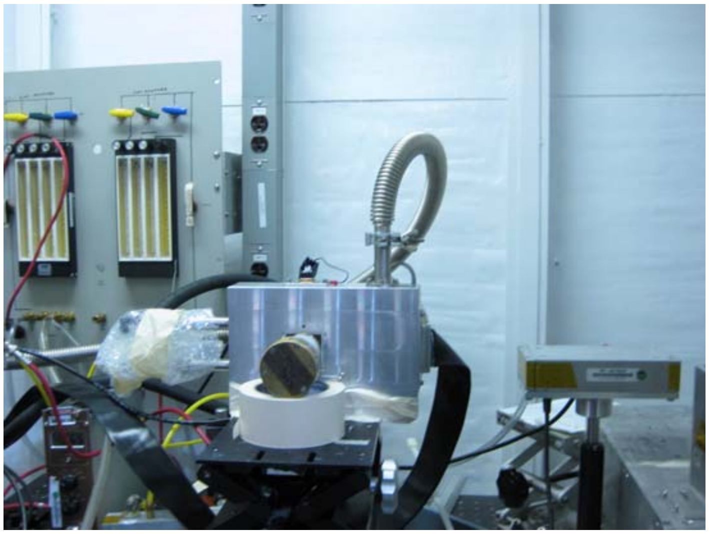

(b)


(c)


Fig. 2.4. Full set-up at X11B for detector testing first with a Fe^{55} radioactive source. Note that compact nature of the new detector in (a) and the support equipment (vacuum pump, chiller and electronic control box (black box)) in (c). The dimensions of the detector housing are 21.4 cm (length) x 14.4 cm (height) x 5.6 cm (Depth) and the weight is 8 lbs making it easily mountable for a large range of spectroscopic and scattering experiments.

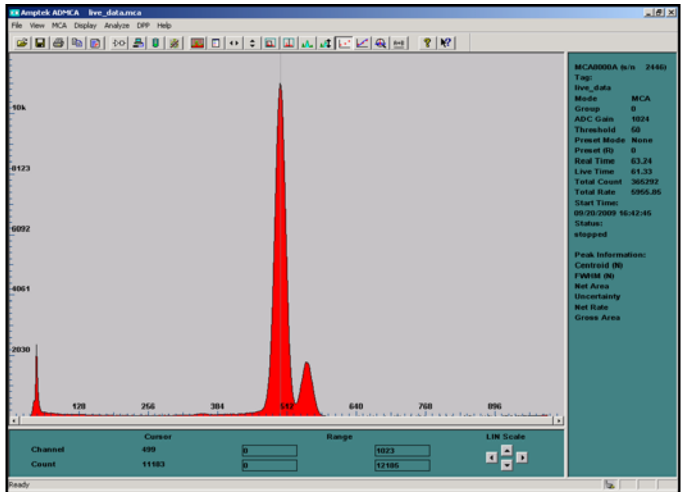

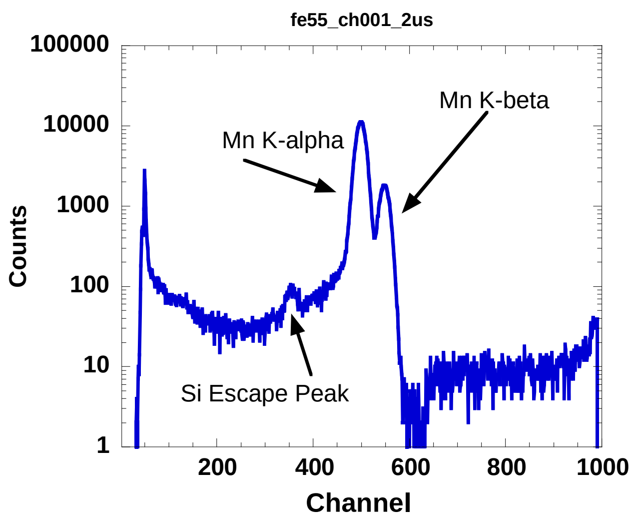

(b)

Fig. 2.5. Typical MCA spectrum of one detector element (Channel 1, upper right quadrant in Fig. 2.3), for signal from Fe^{55} source. At the the count rate of ~6,000 cps the energy resolution of the detector elements is 300 eV for 2 μs shaping time. Main lines shown are the Kα and Kβ lines of the Mn product atoms. The peak at vey low channels corresponds to noise in the detector. The signal is shown on a log scale in (b) accentuating both weak and strong peaks in the spectrum. The estimated peak to background ratio is 400:1

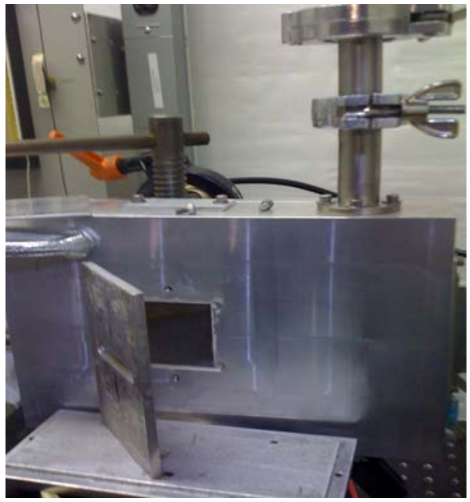

(a)

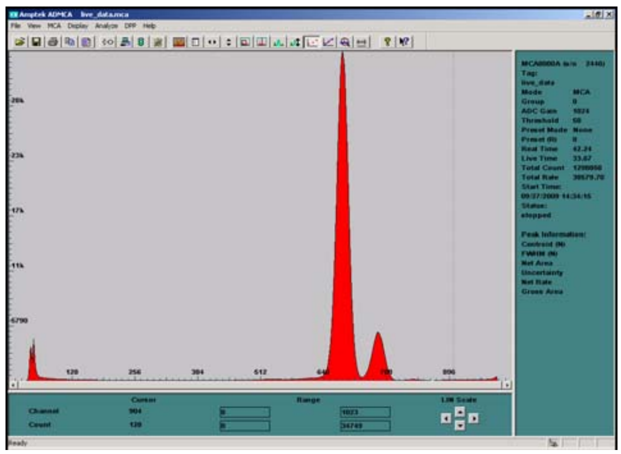

(b)

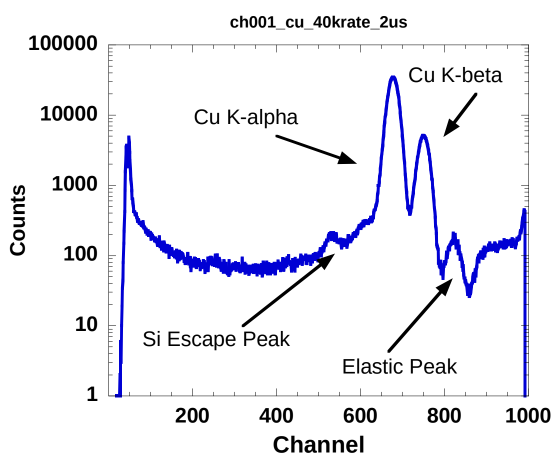

(c)

Fig. 2.6. Setup for Cu fluorescence measurements using a Lytle sample lid shown in (a). The fluorescence foil or film sample was placed at the position of the hole at 45° to the detector. The beam strikes the sample from the right after passing trough an ion chamber. The incident flux on the sample was express in terms of the ion chamber signal (as a voltage converted from the measured current). The incident energy is 9100 eV. In (b) we show the Cu emission spectrum on a linear scale and in (c) the same spectrum on a log scale. The data are for channel 1 with an output rate of ~40,000 cps.

Detector Response to Input Cu Fluorescence
(measured relative to intensity (I0 volts) on Cu Foil sample)

For a shaping time of 2 ms, operating each element at 50,000 cps (or less) keeps operations in the linear regime and gives good energy resolution (~300 to 375 eV) and a total count rate of ~ 50,000 *384 = 19 MHz. Sacrificing resolution (~350 eV, for a broad counting range up to high count rates) by working with 0.5 shaping time yields a total count rate of at least three times higher (> 57 MHz) while remaining in the quasi-linear regime. At this high rate minor dead-time corrections will have to be applied The response to in put counts and peak widths is given in Figs 2.7 and 2.8 MCA profiles for a representative survey of the detector channels is given in Appendix A.

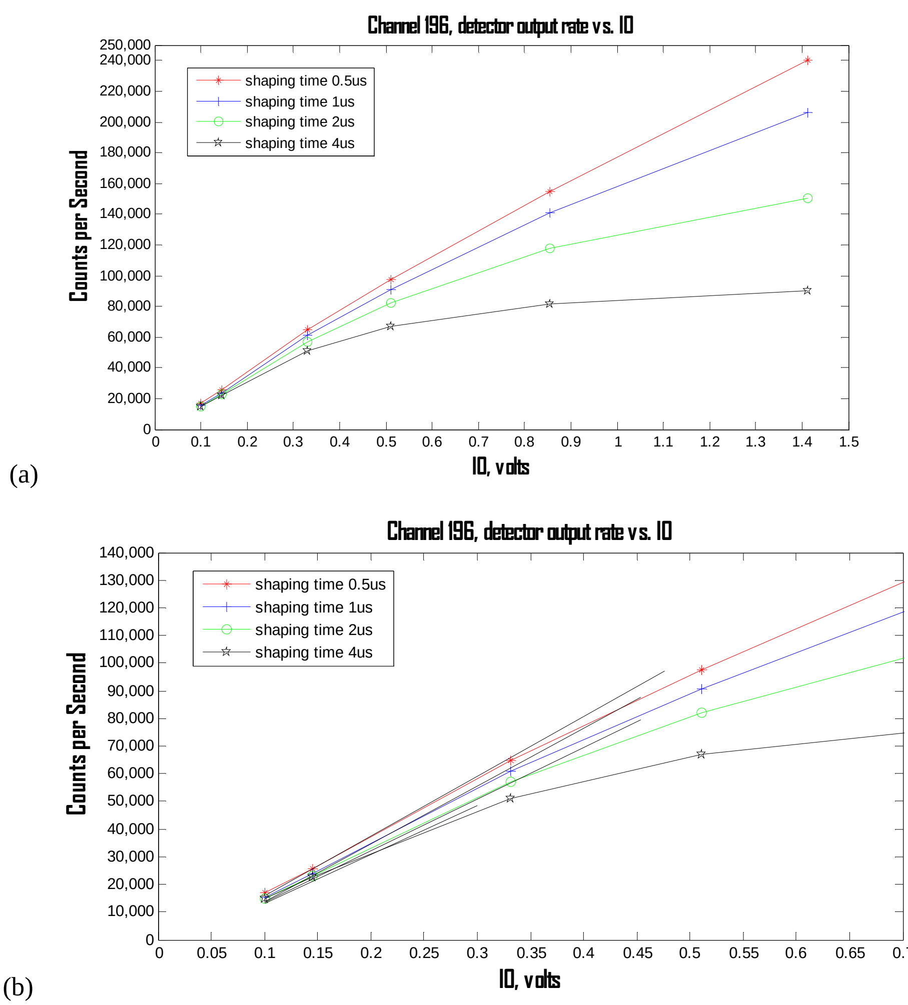

Fig. 2.7 Output counts vs. input fluorescence signal (in terms of incident beam intensity (as I0 voltage) for detector channel 196 (representative channel). The lower panel (b) expands the low flux region. Straight lines serve as guides to the eye. The responses are linear up to ~20,000 and ~50,000 cps for 4 and 2 µs shaping times, respectively. For 1 and 0.5 µs shaping times linearity extends to ~50,000 cps, respectively. With small corrections (dead times) acquisition rates of ~150,000 cps can be obtained for each detector channel at shaping times of 0.5 µs. The incident energy used is 9100 eV.

Detector Cu Kα widths as a function of Input Cu Fluorescence (Measured relative to intensity (I0 volts) on Cu Foil sample)

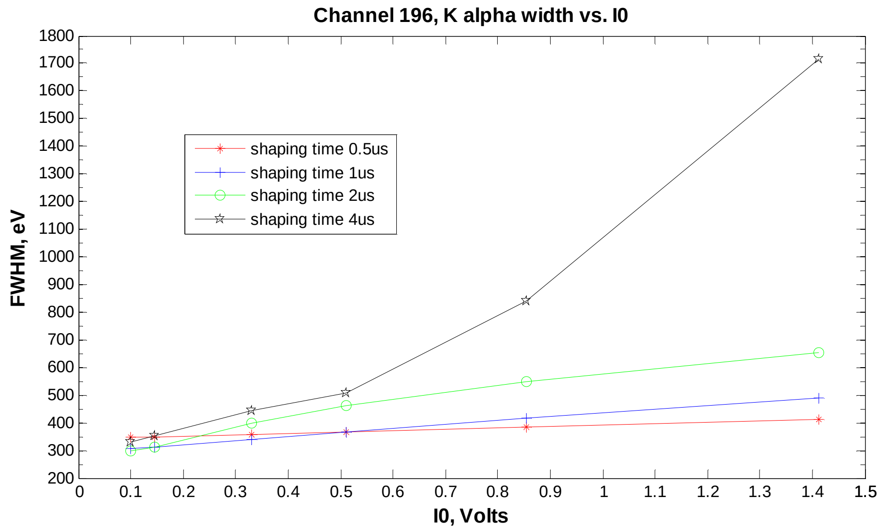

(a)

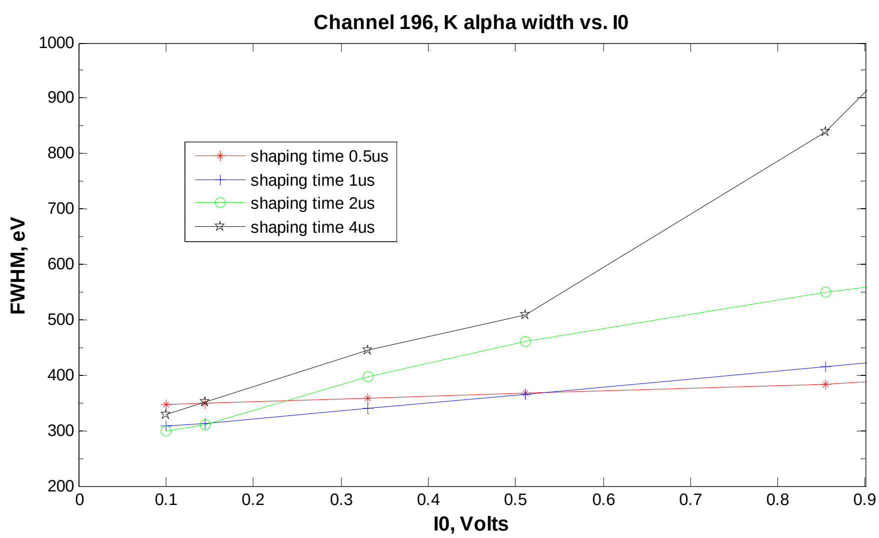

(b)

Fig. 2.8 Cu Ka fluorescence peak width vs. input fluorescence signal (in terms of incident beam intensity (as I0 voltage) for detector channel 196 (representative channel). Panel (b) gives an low region blow up of (a). For a shaping time of 2 μs, a resolution better than ~300 eV is obtained up to 30,000 cps and better than ~375 eV up to 50,000 cps. Interestingly, at 0.5 μs shaping times (red curve), the resolution maintains a value of ~350 eV for output counts up to 200,000 cps with negligible increase.

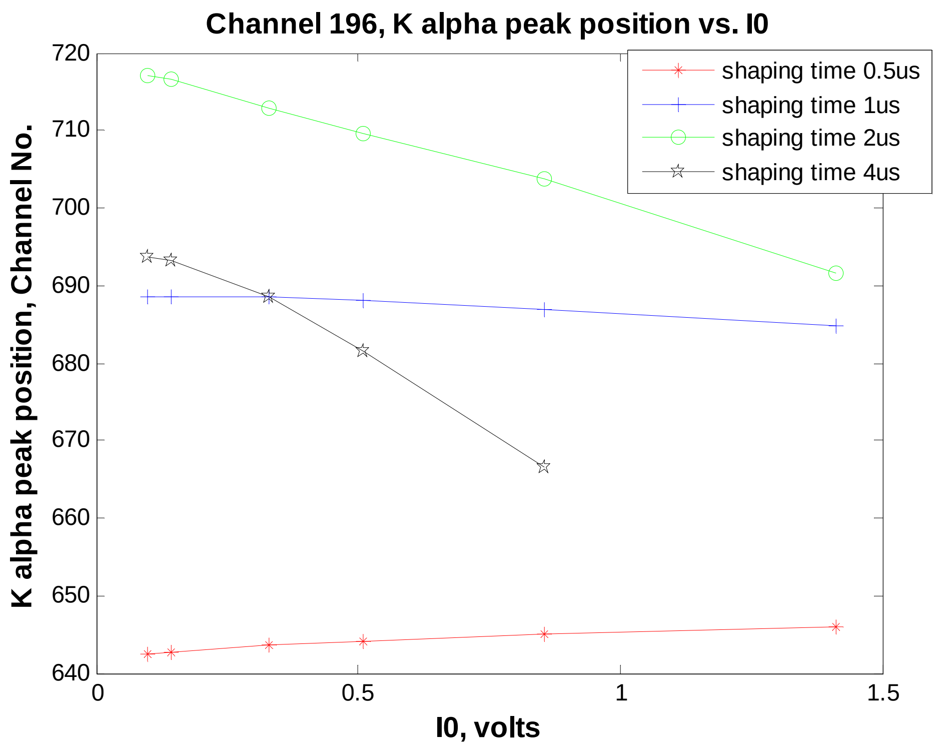

Fig. 2.9 Cu Kα fluorescence peak position (as MCA channel number) vs. input fluorescence signal (in terms of incident beam intensity (as I0 voltage) for detector channel 196 (representative channel). On the y-axis scale a shift of channel number by 1 unit is equivalent to 20 eV. For the 2 μs curve good resolution and position stability will be maintained away from the white line in the XAFS region where is no large change in fluorescence counts (rates below 50,000 cps, see Fig. 2.7). The 0.5 and 1 μs peak positions curves are very stable to very high counting rates on the other hand.

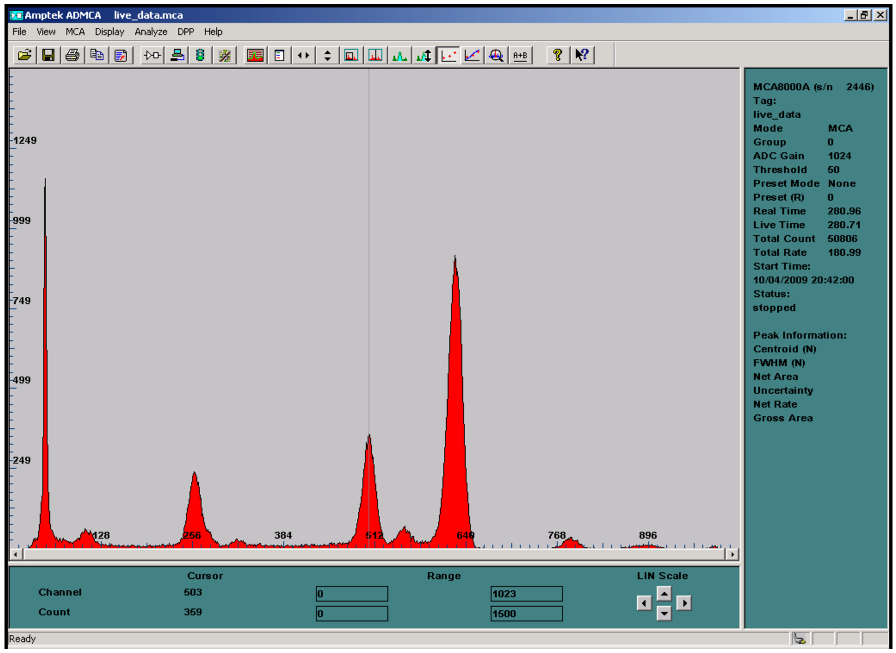

(a)

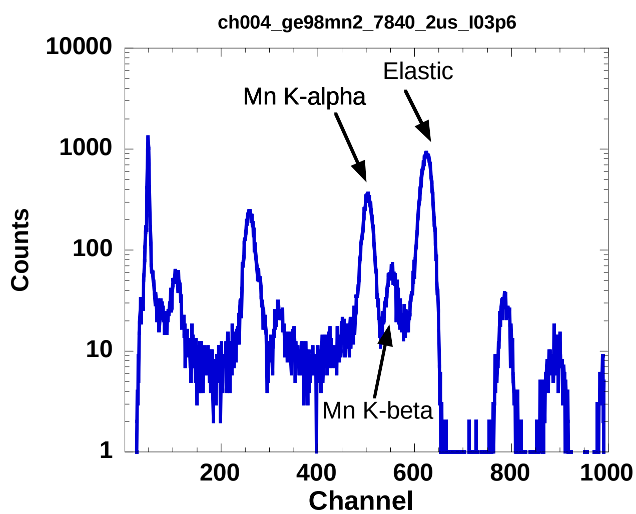

(b)

Fig. 2.10. Real sample measurement (channel 4, 2 μs shaping time). Data taken from 100 nm film of Ge0.98Mn0.02 on GaAs. The MCA spectrum is shown in (a) on a linear scale and in (b) on a log scale. The incident energy is 7840 eV. The emission lines above the main elastic line are excited by hard x-ray contamination of the incident beam by the Si(333) harmonic. Additonal impurity sample lines are also evident at lower energies. Additional emission lines from the sample are also present. The FWHM for the Mn Ka line is 274 eV due to the low counting rates.

(a1) 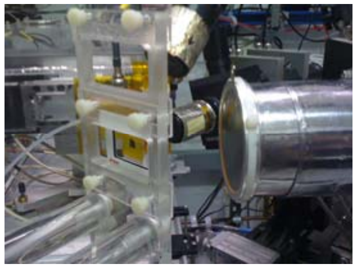 (a2) 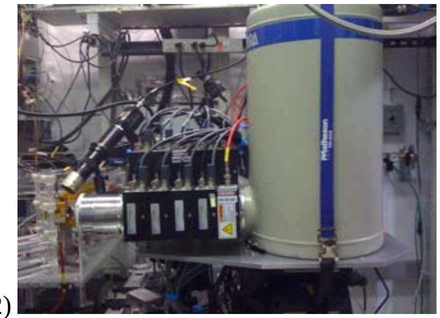

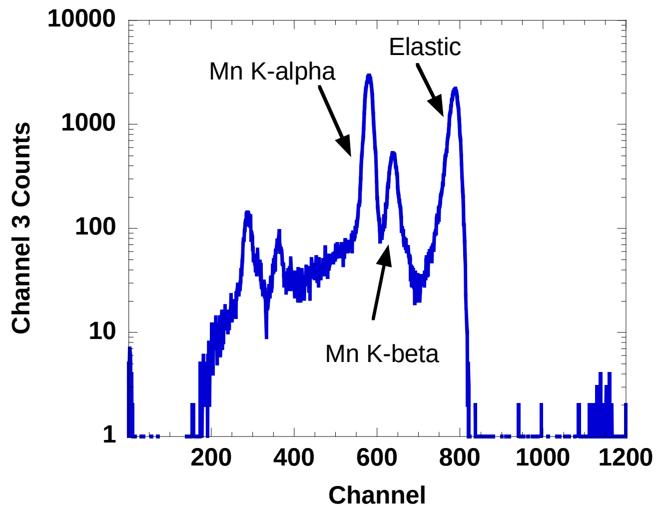

(b)

Fig. 2.11. The X27A Canberra 13-thirteen element Ge detector ((a1) and (a2)) with digital signal processing was used to measure the fluorescence spectrum of the 100 nm Ge0.98Mn0.02 film on a GaAs substrate for comparison with our 384 element detector. The incident energy was set at 9000 eV. The spectrum shown in (b) is from detector 3 (channel 3). As for our 384 element detector additional impurity peaks are also evident. Harmonic content is suppressed in this case due to the use of a Si(311) monochromator. The FWHM for the Mn Ka line is 248 eV as a result of the low input rate.